Calculation of Constant-Energy Surfaces for Copper by the Korringa-Kohn-Rostoker Method*

J. S. FAULKNER, HAROLD L. DAVIS, AND H. W. JOY
Metals and Ceramics Division, Oak Ridge National Laboratory, Oak Ridge, Tennessee
(Received 3 April 1967)

Constant-energy surfaces are calculated for a number of different energies using three different potential functions for copper. Each surface is specified by values for 26 066 radii in **k** space, the radii being calculated with the Korringa-Kohn-Rostoker band-theory method. The Fermi surfaces obtained are used to discuss the available experimental results. Values for the electronic contribution to the low-temperature specific heat that are not clouded by statistical errors or interpolation difficulties are calculated. The density-of-states curve for a range of energies above the *d* bands is calculated using the Chodorow potential. Questions concerning the convergence of the calculation are treated in detail.

I. INTRODUCTION

THE method for investigating electron energy bands that has come to be called the Korringa-Kohn-Rostoker method[1,2] (also the KKR or Green's-function method) has many desirable features, one of these being that it seems to work as well for solids that have complicated band structures as it does for simpler ones. Previous calculations with this method[3,4] have demonstrated its reliability and usefulness, but did not give the detailed information for regions of low symmetry in the Brillouin zone that is desirable for many applications. By a careful treatment of the computational problems that are involved and the use of more modern computers we have developed a technique for obtaining very accurate results by the KKR method in all regions of the Brillouin zone with an expenditure of computer time that is quite modest by band-theory standards. The results of our calculations take the form of numerical representations of constant energy surfaces. Many quantities of interest in solid-state theory are expressed in terms of constant energy surfaces, particularly the Fermi surface.

The KKR method makes use of certain functions, called structure constants, that depend on the crystal structure of the solid under consideration but not on the crystal potential. It has been thought that the calculation of these functions is so difficult that it forms a stumbling block for the application of this method, necessitating the use of tabulated values. We have found, on the contrary, that very fast band-theory calculations can be done which include the generation of structure constants as an integral part of the over-all calculation. This point is discussed further in the following section.

Several band-theory calculations on copper have been published. Our original interest in this material was to test our results against the published values. We soon found, however, that the degree of detail that we obtain for a given potential allows us to clear up a number of questions that remained open concerning the band-theory predictions for quantities of physical interest. In addition, the relative ease with which the results are obtained allows us to investigate the potential dependence of the results by repeating the calculation for several different potentials, and to investigate the convergence of the results in detail.

II. THE KKR METHOD

In most treatments of band theory the electronic states are found by applying the Rayleigh-Ritz variational principle to the one-electron Hamiltonian for the crystal. These treatments differ among themselves in their choice of basis functions. Korringa,[1] on the other hand, considered the scattering relations that must be satisfied for an electron propagating through the crystal as a Bloch wave and showed that they can be made consistent only if the electron's energy E and wave vector $\mathbf{k}$ satisfy a definite relation. This relation was put in the form of a mathematical expression by applying to the electronic problem the dynamical theory of lattice interferences that Ewald used to investigate electromagnetic waves in solids.[5] Kohn and Rostoker,[2] in an independent treatment, set up the scattering problem as an integral equation which was solved by means of a variational theorem. They showed that the expression relating E and $\mathbf{k}$ they obtained is the same as Korringa's.

The derivation of the fundamental equations is explained very clearly in the original papers on this method, and those discussions will not be repeated here. It is necessary to review certain of the ideas involved, however, in order to describe the nature of the present calculations. For simplicity in the discussion, we restrict our attention to systems that have one atom in a unit cell.

Kohn and Rostoker performed some calculations with this method, as did Morse,[6] but the most extensive calculations thus far were done by Ham and Segall, who also discuss certain practical questions concerning the

* Research sponsored by the U. S. Atomic Energy Commission under contract with the Union Carbide Corporation.
[1] J. Korringa, Physica **13**, 392 (1947).
[2] W. Kohn and N. Rostoker, Phys. Rev. **94**, 1111 (1954).
[3] F. S. Ham and B. Segall, Phys. Rev. **124**, 1786 (1961).
[4] B. Segall, Phys. Rev. **125**, 109 (1962).
[5] P. P. Ewald, Ann. Physik **64**, 253 (1921).
[6] P. M. Morse, Proc. Natl. Acad. Sci. (U. S.) **42**, 276 (1956).

method.[3] All of these calculations assume a muffin-tin potential, i.e., a spherically symmetric potential within nonoverlapping spheres of radius R surrounding each atom and zero potential outside the spheres. Calculations on models and real systems indicate that forcing the crystal potential into this form does not harm the reliability of the results.

Within the muffin-tin approximation the wave function inside an atomic sphere can be expanded, for any fixed value of E, in the form

$$\psi=\sum_{l=0}^{l_{\max}}\sum_{m=-l}^{l} i^l C_{lm} R_l(r) Y_{lm}(\theta,\phi), \tag{1}$$

where $Y_{lm}(\theta,\phi)$ is a spherical harmonic and $R_l(r)$ is a nonsingular solution of the radial equation

$$\left[-\frac{1}{r^2}\frac{d}{dr}\left(r^2\frac{d}{dr}\right)+\frac{l(l+1)}{r^2}+V(r)-E\right]R_l(r)=0, \tag{2}$$

with $V(r)$ the potential in the sphere. This expansion becomes exact in the limit as $l_{\max}$ approaches infinity.

References 1 and 2 show that an electron can propagate through the crystal as a Bloch wave with wave vector $\mathbf{k}$ only if the coefficients in Eq. (1), C_{lm}, satisfy a set of simultaneous equations

$$\sum_{l'=0}^{l_{\max}}\sum_{m'=-l'}^{l'} \Lambda_{lm;l'm'} C_{l'm'}=0, \tag{3}$$

where the elements $\Lambda_{lm;l'm'}$ are functions of E and $\mathbf{k}$. Denoting the determinant of these elements by $F(E,\mathbf{k})$, it follows that the desired relation between E and $\mathbf{k}$ for propagating electrons is obtained from the equation

$$F(E,\mathbf{k})=0. \tag{4}$$

This equation cannot be solved analytically, so numerical methods must be used. Two obvious possibilities for searching for the zeros of $F(E,\mathbf{k})$ are to choose particular values of $\mathbf{k}$ and vary E, or to take E constant and search $\mathbf{k}$. We have chosen the latter scheme because we feel that it leads to the most useful form for the band-theory results and also because the equations of the KKR method lend themselves to such a treatment.

For values of E and $\mathbf{k}$ such that Eq. (4) is satisfied the wave function inside the atomic sphere can be found from Eqs. (1) and (3). Outside it can be expanded by matching to the solution at the sphere boundary.

In more detail, the elements defined in Eq. (3) are

$$\Lambda_{lm;l'm'}=g_l[B_{lm;l'm'}+\kappa\delta_{ll'}\delta_{mm'}K_l]g_{l'}, \tag{5}$$

where $\kappa=\sqrt{E}$. In this equation

$$K_l=\frac{n_l'(\kappa R)-n_l(\kappa R)L_l(R)}{j_l'(\kappa R)-j_l(\kappa R)L_l(R)},$$

where $j_l(\kappa R)$ and $n_l(\kappa R)$ are spherical Bessel and Neumann functions, and $L_l(R)$ is the logarithmic derivative of the function $R_l(r)$ introduced in Eq. (1), all of these functions being evaluated at the sphere radius R. For a given potential, K_l depends only on the l value and the energy E. It is the cotangent of the phase shift for scattering from the atomic sphere. The functions

$$g_l=j_l'(\kappa R)-j_l(\kappa R)L_l(R)$$

can be absorbed into the coefficients C_{lm}, although the determinant is numerically smaller if they are left in it.

The $B_{lm;l'm'}$ are

$$B_{lm;l'm'}=4\pi\sum_{LM} C_{lm;l'm'}{}^{LM} D_{LM},$$

where $C_{lm;l'm'}{}^{LM}$ is an integral over spherical harmonics,

$$C_{lm;l'm'}{}^{LM}=\int_0^{2\pi}d\phi\int_0^{\pi}d\theta\,\sin\theta Y_{LM}(\theta,\phi)Y_{lm}(\theta,\phi)Y_{l'm'}(\theta,\phi),$$

and the D_{LM} are functions of E and $\mathbf{k}$ that depend on the crystal structure but not on the potential inside the atomic spheres. These functions, called structure constants, were studied by Ewald[5] who developed a technique for calculating them. The form of the functions used by Ham and Segall[3] is

$$D_{LM}=D_{LM}{}^{(1)}+D_{LM}{}^{(2)}+D_{00}{}^{(3)}\delta_{L0}\delta_{M0}$$

with

$$D_{LM}{}^{(1)}=-(4\pi/\tau)\kappa^{-L}\exp(E/\eta)\times\sum_n\frac{|\mathbf{K}_n+\mathbf{k}|^L\exp[-(\mathbf{K}_n+\mathbf{k})^2/\eta]}{(\mathbf{K}_n+\mathbf{k})^2-E}\times Y_{LM}(\mathbf{K}_n+\mathbf{k}),$$

$$D_{LM}{}^{(2)}=\pi^{-1/2}(-2)^{L+1}i^{L}\kappa^{-L}\sum_s{}'\,r_s{}^L\exp(i\mathbf{k}\cdot\mathbf{r}_s)Y_{LM}(\mathbf{r}_s)\times\int_{\frac{1}{2}\eta^{1/2}}^{\infty}\xi^{2L}\exp-\left[\xi^2 r_s{}^2+\frac{E}{4\xi^2}\right]d\xi,$$

$$D_{00}{}^{(3)}=-\frac{\eta^{1/2}}{2\pi}\sum_{\nu=0}^{\infty}\frac{(E/\eta)^\nu}{\nu!(2\nu-1)}.$$

In these expressions, τ is the volume of a unit cell, $\mathbf{K}_n$ is a reciprocal lattice vector, $\mathbf{r}_s$ is a lattice vector in real space, and the other variables were defined above. The parameter η controls the contribution to the structure constant from the sums in real space and reciprocal space, and Ewald pointed out that a suitable balancing of these contributions leads to the most efficient calculation. Segall and Ham published tables of these structure constants for symmetry directions in the Brillouin zone of bcc and fcc crystals.[7]

[7] B. Segall and F. S. Ham, General Electric Report No. 61-RL-2876G, 1961 (unpublished).

The heart of a fully automated band-theory calculation using the KKR method is the development of fast and accurate computer programs for calculating the structure constants and phase shifts that make up the determinant $F(E,\mathbf{k})$. This eliminates the necessity for explicitly tabulated functions and makes the calculation much more flexible. The details of how this is done are too involved to go into here, but it can be seen from the above formulas that the problem is simplified if E is held fixed and $\mathbf{k}$ is varied. For cubic crystals we choose a number of evenly distributed directions in $\mathbf{k}$ space and vary $\mathbf{k}$ along each of these directions from the center of the Brillouin zone to its surface. The zeros of $F(E,\mathbf{k})$ represent the points at which a line drawn in the direction of search intersects the constant-energy surfaces.

For the copper calculations in this paper we searched 561 directions in 1/48 of the Brillouin zone for each energy, which determines 26 066 separate points on each constant-energy surface. The number of directions searched for a particular E is completely at our disposal, although proportionately more time is required to search more directions. The choice of a particular scheme for defining the directions of search is not critical if a sufficiently large number of directions are used. In an Appendix we describe the scheme used in this work for clarity.

For a particular value of E and direction of $\mathbf{k}$, $F(E,\mathbf{k})$ can be treated as a function of a single variable, the magnitude of $\mathbf{k}$. Our searching pattern for the roots of this function is a parabolic interpolation procedure that registers convergence when the separation between two values of $\mathbf{k}$ that bracket a zero of $F(E,\mathbf{k})$ is less than some ϵ, and then performs a last linear interpolation for the root. In the calculations reported here we chose ϵ to be 10^{-3} except in the neighborhood of points where the line of search crosses a free-electron energy surface and the structure constants are singular. In those regions $F(E,\mathbf{k})$ varies rapidly and we used $\epsilon=10^{-4}$. These choices assure that, as far as the search procedure is concerned, the roots are correct to at least four figures.

There are two separate convergence problems in the KKR method, the truncation of the structure-constant series and the choice of $l_{\max}$. We have included enough terms in the structure constants to insure that inaccuracies from that source cannot be detected by our search procedure. Our experience corroborates the evidence of Ham and Segall that the KKR method converges very rapidly with increasing $l_{\max}$. Calculations carried out on copper for $l_{\max}$ equal to two and four are discussed in Sec. III. It is found that results for $l_{\max}=2$ are sufficiently accurate for all applications.

The practical advantage obtained from focusing attention on high-symmetry points in the Brillouin zone and using group theory, as is often done in band-theory calculations, is the reduction in the size of the determinant that must be evaluated. This is desired not only because the number of elements that must be calculated is reduced but also because the evaluation of a large determinant is a time-consuming process even after its elements are known. The most important consequence of the good convergence of the KKR method for small values of $l_{\max}$ arises from the fact that the order of the determinant $F(E,\mathbf{k})$ is $(l_{\max}+1)^2$ as can be seen from Eq. (3). Since the KKR method automatically leads to relatively small determinants and the technique we have developed for calculating the elements is very fast, we have found no necessity for group theory to speed up calculations. We can thus search the directions of $\mathbf{k}$ space that we need for the proper specification of constant energy surfaces without over-emphasizing the lines of high symmetry.

Another method for band-theory calculations that shares many of the advantages of the KKR method is the augmented-plane-wave (APW) method suggested by Slater[8] and developed by him and his students. A comparison of certain formal aspects of these two methods has been made by Johnson[9] and by Slater.[10] An interesting point that they discuss is the fact that although both methods normally make use of the muffin-tin potential and the radial functions defined in Eq. (2), the (APW) method requires very much larger values of $l_{\max}$ for convergence. The order of the determinants that occur in the APW method is not determined by $l_{\max}$, but instead is given by the number of basis functions that must be used. This leads to rather large determinants and necessitates the use of group theory to obtain convergent results with a reasonable expenditure of computer time. Some constant-energy calculations with the APW method were carried out by Loucks,[11] but most of the calculations with this method have used constant-$\mathbf{k}$ searches. The calculations with the APW method on copper by Burdick[12] and those done by Segall[4] using the KKR method show that the two methods give the same results for specific eigenvalues when they are carried out to convergence. The differences between the values for certain quantities that we give below and the ones that Burdick and Segall obtained using essentially the same potential arise because we make use of the constant energy surfaces that we are able to calculate.

III. CALCULATIONS ON COPPER

There is nothing novel about the idea of focusing attention on constant-energy surfaces in the calculation of quantities of interest from band theory. In simple cases, such as the free-electron model, it is done automatically. For more realistic band theories, however, the practical difficulties involved with obtaining sufficient detail in nonsymmetry directions has led to the development of alternative methods for calculating these quantities. In the preceding section we discussed

[8] J. C. Slater, Phys. Rev. **51**, 846 (1937).
[9] K. H. Johnson, Phys. Rev. **150**, 429 (1966).
[10] J. C. Slater, Phys. Rev. **145**, 599 (1966).
[11] T. L. Loucks, Phys. Rev. **139**, A1181 (1965).
[12] G. A. Burdick, Phys. Rev. **129**, 138 (1962).

how the KKR method can be used for calculating constant-energy surfaces, and in this section we show how these surfaces are used to obtain information about copper.

One of the potential functions that we use, which we call V_{I}, was obtained by fitting to the values for the potential function proposed for copper by Chodorow in 1939 that are given in Ref. 12. Some small differences may have been introduced in this process, but we believe that V_{I} is essentially the Chodorow potential.[13] Two other potential functions were generated from atomic Hartree-Fock wave functions by a method that has been widely used in band-theory calculations.[14] In one of these, which we call V_{II}, the copper wave functions were calculated by Watson.[15] This potential should be about the same as one used by Mattheiss[16] in a calculation along one symmetry axis that was done in connection with some other work. In the other, called V_{III}, the wave functions were obtained from Herman and Skillman's tabulations.[17]

The first step in the calculations with a particular potential function is to survey the bands of interest by calculating $E(\mathbf{k})$ curves along symmetry directions for a wide range of energies. This makes it possible to obtain an orientation with respect to the general features of the bands.

The energy bands of transition metals are frequently described by grouping together those portions of the bands that behave like the sp band of simple metals, and then referring to the flat bands that lie across the sp band and hybridize with it as d bands. Surveys along the symmetry axes with the potentials described above show that the shapes of the sp bands are not sensitive to the potential used, but the positions of the d bands relative to the sp bands do vary with potential. The d bands appear highest relative to the sp band when V_{II} is used in the calculation, they are lower when V_{I} is used, and they are lowest when V_{III} is used.

In Table I we show the values that we have calculated with these potentials for the energy of the lowest band state above the rare-gas core $E(\Gamma_1)$, the energy at which the conduction band makes contact with the hexagonal faces of the Brillouin zone $E(L_{2'})$, and the energy at which the conduction band makes contact with the square faces, $E(X_{4'})$. Values for the Fermi energy calculated by the method described below are also shown. In this table, and throughout the following, all other energies are measured from the lowest band energy $E(\Gamma_1)$ calculated with the potential under consideration. Energies as calculated can be obtained by adding $E(\Gamma_1)$ to the quoted values.

TABLE I. The energies of certain special points from the energy bands calculated with different potentials. The unit is rydbergs, and the energies of the other points are measured from $E(\Gamma_1)$.

Potential	$E(\Gamma_1)$	$E(L_{2'})$	$E(X_{4'})$	E_f
V_{I} $l_{\max}=2$	−1.0468	0.6145	0.8156	0.6685
V_{I} $l_{\max}=4$	−1.0468	0.6112	0.8081	0.6672
Chodorow[a]	−1.043	0.614	0.808	0.659
V_{II}	−1.1471	0.5903	0.7995	0.6796
V_{III}	−23.990	0.6120	0.8044	0.5930

[a] From the APW calculation of Ref. 12.

It can be seen from Table I that when V_{III} is used, E_f is less than $E(L_{2'})$. This means that the Fermi surface calculated with this potential does not make contact with the hexagonal faces of the Brillouin zone, which disagrees with the experimental results described below. The results obtained using V_{I} and V_{II} are more reasonable, and we will focus our attention on these potentials for comparisons with experiments.

The calculations described above were carried out using $l_{\max}=2$. In order to check the convergence of the results, a number of calculations have been done using the potential function V_{I} with larger values of $l_{\max}$. Some of the values obtained are shown in Table I. In going from $l_{\max}=2$ to $l_{\max}=4$, $E(\Gamma_1)$ changes by less than 10^{-4} Ry. For all eigenvalues tested the change was less than 10^{-2} Ry. The changes seem to be greater for points on the symmetry axes than for general points. With such good convergence we use $l_{\max}=2$ for most of our calculations, although we did calculate the Fermi surface and one constant-energy surface on either side of it using V_{I} and $l_{\max}=4$ for additional checks.

Since the potential function V_{I} is essentially the Chodorow potential used in Burdick's APW calculations,[12] we have compared our results with his. As is illustrated by the values in Table I, the differences for specific eigenvalues arise in the third decimal place. This is the kind of agreement that Burdick and Segall[4] had already demonstrated between the APW and KKR methods. The errors that we introduce by using $l_{\max}=2$ seem to be at least as small as the truncation errors in Burdick's calculation, which is in agreement with the general considerations of Johnson[9] on this point.

If a constant-energy surface is calculated for some energy E then twice the volume inside of this surface divided by the volume of the Brillouin zone gives the number of states per atom in that band having an energy less than E. If there is only one band at E then this quantity is the integrated density of states $M(E)$. If there is more than one band at E it is necessary to sort out the points obtained from the constant-energy search with respect to the various bands involved. The volume inside of each surface is calculated separately and $M(E)$ is obtained from the sum of the volumes. It is necessary to take care that the regions of k space

[13] Throughout this paper we use the value for the lattice constant of copper that is quoted in Ref. 12, $a=6.83087$ a.u.
[14] L. F. Mattheiss, Phys. Rev. 133, A1399 (1964).
[15] R. E. Watson, Phys. Rev. 119, 1934 (1960).
[16] L. F. Mattheiss, Phys. Rev. 134, A970 (1964).
[17] F. Herman and S. Skillman, *Atomic Structure Calculations* (Prentice-Hall, Inc., Englewood Cliffs, New Jersey, 1963).

TABLE II. The integrated density of states $M(E)$ and density of states $\rho(E)$ calculated for a number of energies using the potential function V_I with $l_{max}=2$.

E (Ry)	$M(E)$	$\rho(E)$	E (Ry)	$M(E)$	$\rho(E)$
0.51785	0.39878	4.36	0.72090	1.18444	2.88
0.53477	0.48090	3.88	0.73782	1.24141	2.82
0.55169	0.55483	3.55	0.75475	1.29727	2.77
0.56861	0.62369	3.35	0.77167	1.35202	2.71
0.58553	0.68941	3.23	0.78859	1.40578	2.65
0.59399	0.72154	3.21	0.79705	1.43261	2.62
0.60245	0.75344	3.18	0.80551	1.45886	2.60
0.61091	0.78529	3.20	0.80720	1.46408	2.61
0.61261	0.79169	3.21	0.80889	1.46932	2.63
0.61430	0.79812	3.22	0.81059	1.47461	2.66
0.61599	0.80461	3.25	0.81228	1.47996	2.69
0.61768	0.81109	3.24	0.81397	1.48539	2.74
0.61937	0.81758	3.23	0.81566	1.49089	2.72
0.62783	0.84976	3.20	0.81735	1.49629	2.69
0.63630	0.88159	3.17	0.81905	1.50165	2.66
0.64476	0.91314	3.14	0.82074	1.50697	2.65
0.65322	0.94444	3.11	0.82243	1.51222	2.64
0.66168	0.97542	3.09	0.83089	1.53850	2.62
0.66675	0.99392	3.07	0.83935	1.56451	2.56
0.66845	1.00002	3.06	0.85627	1.61448	2.42
0.67014	1.00613	3.06	0.87320	1.66108	2.28
0.67860	1.03655	3.03	0.89012	1.70575	2.15
0.67806	1.06673	3.00	0.90704	1.74760	2.05
0.70398	1.12608	2.94			

separated by a constant-energy surface are correctly identified as being inside or outside the surface, since many bands have their energy minima at points other than the center of the Brillouin zone. An over-all survey of the general behavior of the bands and a comparison of neighboring energy surfaces for small changes in E are helpful in making this identification.

If n is the number of electrons per atom that must be put into band states, then the Fermi energy E_f is defined by the equation $M(E_f)=n$. Clearly the Fermi energy can be found very accurately by calculating $M(E)$ for several energies in the neighborhood of E_f. The density of states for the system is defined as the derivative of $M(E)$ with respect to energy, $\rho(E)=dM/dE$.

In copper there is only one band for energies in the neighborhood of the Fermi energy. The constant-energy surfaces for this band were calculated for a number of energies above the d bands using V_I and $l_{max}=2$. The enclosed volumes were calculated by a simple numerical integration technique. This technique and our reasons for believing that it leads to a function $M(E)$ that is accurate to approximately four decimal places are discussed in the Appendix. The density-of-states function $\rho(E)$ was calculated by fitting the calculated values of $M(E)$ to polynomials within limited energy intervals and differentiating the polynomials. We feel that this procedure leads to values for $\rho(E)$ that are accurate to three figures. Values for these functions are given in Table II for all of the energies at which the constant energy surfaces were calculated. It can be seen that the intervals between successive energies are not equal. One of the advantages in this technique is that greater detail can easily be obtained in energy regions where this is desirable because the functions are varying rapidly or for some other reason.

There are eleven electrons in copper outside of the rare-gas core that must be fitted into the calculated bands. Ten of these go into the five bands which fall completely below the energies that we are considering. Thus, the energy for which $M(E)=1.0$ is the Fermi energy. The value of 0.6685 Ry obtained from Table II differs from the value of 0.659 Ry obtained by Burdick and 0.658 Ry obtained by Segall partly because of small differences in the eigenvalues but also because it is more difficult to obtain an accurate Fermi energy from their data.

In Table III we give three values of the integrated density of states calculated using V_I and $l_{max}=4$, V_{II}, and V_{III}. These results justify the Fermi energies quoted in Table I and can also be used to calculate a density of states at the Fermi energy.

The density of states, integrated density of states, and Fermi energy represent only a small part of the information that is contained in the complete numerical representations of constant energy surfaces that have been calculated. The dimensions of the Fermi surface measured by the magnetoacoustic effect and the cross-sectional areas of planes passing through the Fermi surface measured by the de Haas–van Alphen effect are easily and accurately found for a given potential from the numerical representation of that surface. The rate of change with energy of cross-sectional areas of the Fermi surface measured by cyclotron resonance experiments can be obtained by using the Fermi surface and another surface calculated for an energy sufficiently close to E_f. The results of calculations with V_I and V_{II} of certain quantities that are measured in these experiments are shown in Table IV. Calculations with V_I and $l_{max}=4$ are shown to demonstrate convergence. With the 26 066 points on the Fermi surface that we have obtained more elaborate comparisons could be made, but these are sufficient for our present purposes.

A searching procedure that is different from the one described in the Appendix is used to investigate the neck where the Fermi surface is in contact with a hexagonal face of the Brillouin zone. Lines of search lie in the plane of this face and $\mathbf{k}$ is varied from its center to its edge in a number of directions. The distances from the center of the hexagonal face to the points where the lines of search cross the Fermi surface are calculated to at least four-figure accuracy for a

TABLE III. The integrated density of states $M(E)$ calculated for three energies using different potential functions.

$V_I, l_{max}=4$		V_{II}		V_{III}	
E (Ry)	$M(E)$	E (Ry)	$M(E)$	E (Ry)	$M(E)$
0.66169	0.97981	0.67621	0.98584	0.58884	0.98771
0.66723	0.99993	0.67960	0.99992	0.59299	0.99999
0.67015	1.01062	0.68467	1.02097	0.59730	1.01290

TABLE IV. The comparison of certain quantities that we have calculated with the experimental results discussed in the text.

	Fermi-surface radii (dimensionless)			de Haas–van Alphen frequencies (10^8 G)			Cyclotron masses (dimensionless)			Low-temperature specific-heat coefficient (mJ/g-atom deg^2)
	k_{100}	k_{110}	k_N	F_B	F_D	F_N	$(m^*/m_e)_B$	$(m^*/m_e)_D$	$(m^*/m_e)_N$	γ
V_{I} $l_{\max}=2$	1.0501	0.9553	0.1783	5.957	2.510	0.193	1.21	1.13	0.38	0.629
V_{I} $l_{\max}=4$	1.0530	0.9544	0.1808	5.960	2.504	0.199	1.22	1.12	0.38	0.631
V_{II}	1.0658	0.9426	0.2146	5.920	2.462	0.280	1.43	1.23	0.42	0.720
Experiment	1.036	0.956	0.195	6.0337	2.5203	0.2187	1.37	1.29	0.46	0.697

given case. In addition to finding accurate parameters for the neck we have also shown that the neck is circular. Radii calculated using V_{I} and V_{II} show no change with direction to within the accuracy of the calculation. Burdick's less detailed results[12] indicated the possibility of a noncircular neck, but the magnetoacoustic and de Haas–van Alphen experiments are consistent with a circular one.

The most direct measurements of the radii of the Fermi surface come from the magnetoacoustic effect. The radii in the ⟨100⟩ and ⟨110⟩ directions, k_{100} and k_{110}, and the neck radius k_N expressed as ratios of the calculated values to the radius of the free-electron sphere are compared with Bohm and Easterling's experimental values[18] in Table IV. The neck radius obtained using V_{II} is too large, and also the value for k_{100} shows that this Fermi surface is pulled out too far in the direction of the square face. A more detailed investigation of the radii in the {100} and {110} planes shows that the radii of the Fermi surface calculated with V_{I} agree with Bohm and Easterling's measurements to within experimental error for most directions that they could measure directly, except for those rather close to the neck which are too small. Previous calculations with the Chodorow potential agree with our value for k_{100}, but agree less well for k_{110} and k_N. The Fermi surface obtained using V_{II} is quite similar to the one advanced by Roaf[19] to fit the de Haas–van Alphen results of Shoenberg.[20]

The de Haas–van Alphen frequencies are calculated from the formula

$$F=chA/4\pi^2e\,,$$

where A is the central extremal area perpendicular to the ⟨100⟩ directions for F_B shown in Table IV, it is the dog's-bone area for F_D, and the neck area for F_N. The calculations are compared with the experimental results of Joseph, Thorsen, Gertner, and Valby.[21] Dr. I. M. Templeton is quoted by Zornberg and Mueller[22] to the effect that his experiments indicate that the experimental frequencies we are using may be 0.6% too large. If they are changed by the amount, then the calculations with V_{I} yield reasonable values for F_B and F_D, but the neck area is too small as was already indicated by the magnetoacoustic results. The differences between the frequencies calculated using V_{II} and experiment are also consistent with the magnetoacoustic results, indicating too large a neck area and too much distortion in the belly.

The ratio of cyclotron masses to the mass of the electron is given by

$$\frac{m^*}{m_e}=\frac{\hbar^2}{2\pi m_e}\frac{\partial A}{\partial E}.$$

The subscripts on the m^*/m_e given in Table IV refer to the same extremal cross-sectional areas that were used in connection with the de Haas–van Alphen results. The experimental values are obtained from the cyclotron resonance experiments of Koch, Stradling, and Kip.[23] It is seen that the agreement between the calculations and experiment is not as good as in the preceding cases. Our values using V_{I} agree with the results calculated by Segall[4] with approximately the same potential, but the uncertainties in our calculation are much smaller.

IV. DISCUSSION OF RESULTS FOR COPPER

The above data seem to indicate that the best potential for copper, as far as states very near the Fermi surface are concerned, would be similar to V_{I} but modified in the direction of V_{II}. This means, effectively, that the d bands should be higher than those obtained using V_{I} but lower than the ones obtained using V_{II}. Such a change would make the neck bigger, hopefully without distorting the belly too much. The agreement with the cyclotron resonance experiments should also

[18] H. V. Bohm and V. J. Easterling, Phys. Rev. **128**, 1021 (1962).
[19] D. J. Roaf, Phil. Trans. Roy. Soc. London **255**, 135 (1962).
[20] D. Shoenberg, Phil. Trans. Roy. Soc. London **255**, 85 (1962).
[21] A. S. Joseph, A. C. Thorsen, E. Gertner, and L. E. Valby, Phys. Rev. **148**, 569 (1966).
[22] E. I. Zornberg and F. M. Mueller, Phys. Rev. **151**, 557 (1966).
[23] J. F. Koch, R. A. Stradling, and A. F. Kip, Phys. Rev. **133**, A240 (1964).

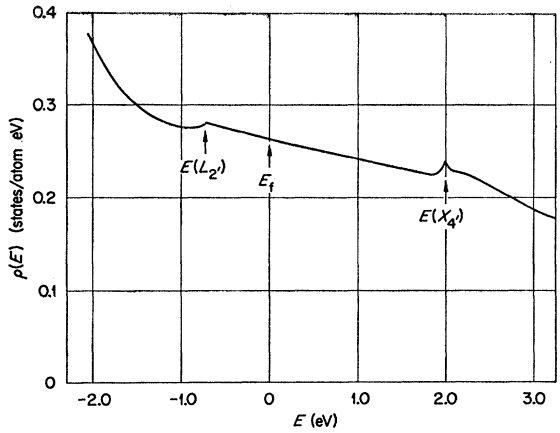

FIG. 1. The density of states versus energy obtained using the potential function V_{I} with $l_{\max}=2$.

be improved. Of course, one cannot shift values around at random by this means. For example, it is no doubt impossible to find a muffin-tin potential that will give a Fermi surface that has the larger neck area required by the de Haas–van Alphen frequency F_N without making the calculated F_B and F_D smaller than the frequencies predicted using V_{I}. This lends theoretical support to the suggestion that the experimental values of Ref. 20 are slightly larger than they should be. Since we are interested in band theory rather than in just fitting Fermi-surface data, the critical question for such an adjusted potential would be whether or not the position of the d bands, the critical points $E(L_{2'})$ and $E(X_{4'})$ and other features that give information about states away from the Fermi energy could be made consistent with photoemission experiments, optical experiments, and other experiments that measure these features. In the following section we discuss the possibilities for obtaining such a potential.

The coefficient of T in the electronic contribution to specific heat is given by

$$\gamma=\tfrac{1}{3}\pi^2k^2\rho(E_f),$$

where k is Boltzmann's constant and $\rho(E_f)$ is the density of states at the Fermi energy. This density of states has been calculated to three-figure accuracy for a given potential and $l_{\max}$, and the resulting γ's are compared with the experimental value of Kneip, Betterton, and Scarbrough[24] in Table IV. The comparison of the values 0.629 and 0.631 mJ/g atom deg^2 calculated using V_{I} with $l_{\max}=2$ and $l_{\max}=4$ shows that errors in the calculated values for a given potential can conservatively be estimated as less than 1%. Segall[4] used an interpolation scheme to obtain $\gamma=0.59$ mJ/g-atom deg^2, and Burdick's[12] histogram gives a value of approximately 0.50 mJ/g-atom deg^2 for the Chodorow potential. Since our accurate calculations give a value for γ that is 10% below the experimental value when V_{I} is used and 3% above when V_{II} is used, it is likely that a potential which leads to a Fermi surface in better agreement with the data will give a value for γ that is even closer to the measurement. This leaves a portion of γ to be explained by electron-phonon interactions that is small in comparison with estimates that have been made for other materials.[25]

The data in Table II have been used to plot the density of states versus energy shown in Fig. 1. The units have been changed to states per eV versus eV, the energy being measured relative to the Fermi energy, to facilitate comparison with experiment. The large values of $\rho(E)$ for low energies arise from the distortion of the conduction band at those energies, since the range of energies shown here is above the d bands. To our knowledge, this is the first time that the density of states for a metal having d bands has been calculated to this accuracy and in this much detail on the basis of a realistic band theory without the use of interpolation schemes for the bands, even over a restricted range of energies. We might point out that our programs will work for the d bands although the investigation is more expensive.

This portion of the density-of-states curve for copper has figured prominently in discussions of alloys.[26] The peaks in the curve at $E(L_{2'})$ and $E(X_{4'})$ are smaller than has generally been assumed in those discussions. The density of states is seen to be a linear function of energy over a rather wide range of energies in the neighborhood of E_f. Attempts have been made to investigate this function by alloying polyvalent metals with copper and measuring the change in γ. According to the rigid-band model, the Fermi energy of such an alloy ϵ_f can be found on the assumption that the extra electrons added to the system fill the states that have been calculated for copper. Thus, if $M(E)$ is the integrated density-of-states function for pure copper, the Fermi energy for the alloy can be found from $M(\epsilon_f)=e/a$, where e/a is the average number of electrons per atom. The slope $d\gamma/d(e/a)$ can be calculated from our data, but the experiments generally give the opposite sign from this calculation.[27]

Berglund and Spicer[28] have made photoemission studies on copper that can be interpreted to give a density-of-states function. Their Fig. 16 shows the peaks at $E(L_{2'})$ and $E(X_{4'})$, but they are much larger than our calculated ones. These results can probably be explained on the basis that the transition probabilities are not the same for all states in the conduction band, but the positions for these peaks that we find are not consistent with their results. Our calculations with V_{I} and V_{II} lead to values of approximately 2.0 eV and 1.6 eV for $E(X_{4'})-E_f$, which agrees reasonably well with

[24] G. D. Kneip, J. O. Betterton, and J. O. Scarbrough, Phys. Rev. **130**, 1687 (1963).

[25] N. W. Ashcroft and J. W. Wilkins, Phys. Letters **14**, 285 (1965).

[26] H. Jones, Proc. Phys. Soc. (London) **49**, 250 (1937); Phys. Rev. **134**, A958 (1964).

[27] L. C. Clune and B. A. Green, Phys. Rev. **144**, 525 (1966).

[28] C. N. Berglund and W. E. Spicer, Phys. Rev. **136**, A1044 (1964).

Berglund and Spicer's value of 1.8 eV. We get 0.75 eV and 1.2 eV for $E_f - E(L_{2'})$, however, and since the larger calculated value is obtained using V_{II} it is hard to see how a potential function that can give predictions which agree with the data on the Fermi surface can yield a value for this separation as small as the 0.35 eV they measure. Although we did not calculate the density of states in the d-band region, we can see from our survey along symmetry axes that the d bands calculated with V_I fall in the interval between 2.1 and 5.6 eV below the Fermi energy, while those calculated with V_{II} fall in the interval between 1.7 and 5.1 eV. The large peak attributed to the d bands by Berglund and Spicer seems to agree more closely with the results obtained using V_I.

One can argue that our calculation does not give the density of states directly, and since we must obtain this function from its integral a narrow but high peak would escape our notice. The data in Table II can be used directly to calculate the area under the density-of-states curve for various energy intervals in the neighborhood of the critical points to a definite number of significant figures, however, and this measure of the size of the peaks is more relevant to most applications than is their maximum heights. We know from the Fermi surface and specific-heat data that the Chodorow potential used to calculate $\rho(E)$ is not optimum, but it is hard to believe that the small changes in potential that are required to improve the agreement with those data will lead to radically different results for size of the peaks.

V. GENERAL DISCUSSION

It might be said that our application of the KKR method gives more accuracy than is needed since the potential functions that are put into the calculation do not merit such a detailed investigation. We feel that the preceding work shows that the elimination of certain ambiguities in the band-theory results makes it possible to gain a clearer understanding of the potential problem and gives a useful estimate for the magnitude of corrections that must be made on the basis of theories that go beyond band theory.

Either V_I or V_{II} give results for states in the neighborhood of the Fermi surface that are in reasonable agreement with experiments. The agreement for states in other energy regions is less satisfactory, but at the present time the experiments that give information about such states are more difficult to carry out and to interpret.

It may be that a self-consistent calculation would give the small corrections to the potential function that the experiments seem to require. Another possibility is that a potential function that is adjusted to give a good fit to all of the relevant experimental data will automatically include the class of many-body effects that can be described in terms of noninteracting quasiparticles. If this latter possibility proves true, then the theory for calculating potential functions from first principles will require further development. The problem of carrying out a self-consistent band-theory calculation in the true Hartree-Fock sense is a very difficult one, especially if it is desired to go beyond the relatively simple assumptions used to treat the exchange potential. As progress is made in the speed and accuracy of band-theory calculations, the approach to true self-consistency should no doubt be pursued, at least until it becomes clear whether or not this is the correct line to follow. In any case, the results of this work are consistent with the general experience gained from other investigations that band-theory calculations will give a great deal of information that is useful to solid-state physics even when the potential function is obtained from a simple recipe, if sufficient care is taken to check on the potential dependence of the results.

We feel that the present calculations establish that the KKR method is a very powerful tool for investigating band states, particularly for the nonsymmetry directions.[29] All of these calculations were carried out with a program that gives $E(\mathbf{k})$ for systems having one atom per unit cell. These programs have been generalized to treat systems having more than one atom per unit cell, and programs to give wave functions and to treat relativistic effects are being developed.

APPENDIX: THE SEARCHING PATTERN

As is discussed in Sec. II, the radii of constant-energy surfaces are found by searching for the zeros of the determinant of Eq (4), $F(E,\mathbf{k})$, along a number of lines in $\mathbf{k}$ space.

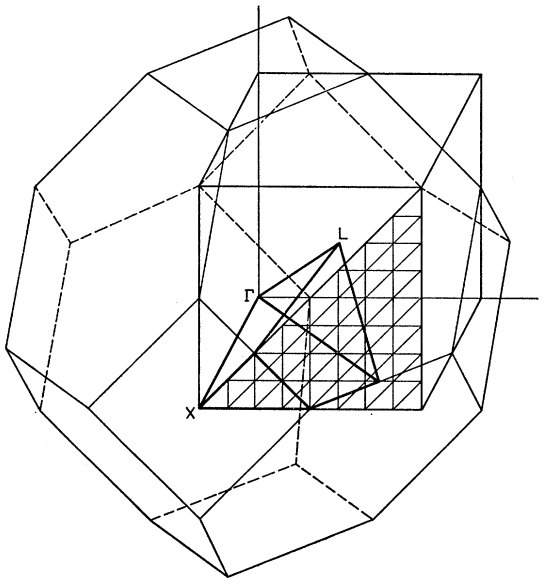

FIG. 2. The mesh that is used to define directions in $\mathbf{k}$ space for fcc crystals.

[29] If the demand is not too great, we can make available to those who have a use for them decks of IBM cards that contain all of the information concerning points on the Fermi surface, and perhaps other constant-energy surfaces, which we have calculated.

Setting up a grid in the plane of the square face of the Brillouin zone as shown in Fig. 2, the lines that connect the point Γ with the points of intersection of the grid can be used as the lines of search. From symmetry considerations it is known that it is sufficient to carry out calculations only in the region of the Brillouin zone set off by heavy lines in the figures which contains 1/48 of the volume of the zone. If N is the number of intervals that a side of the grid is divided into, then the number of lines passing through this region is given by $\frac{1}{2}(N+1)(N+2)$. By searching this set of directions and then using the symmetry of the constant energy surfaces, a total of $24(N-1)(N+3)+26$ distinct points can be found for each surface. In the calculations reported here the value 32 is used for N. Such a mesh leads to the calculation of 561 points on the portion of the constant-energy surface that lies in the 1/48 of the Brillouin zone, and they define 26 066 points on the total surface.

If a constant-energy surface is simply connected its volume can be obtained by adding up the volumes of tetrahedra which have one vertex at Γ and whose edges are the radii of the surface in three neighboring directions. To check the accuracy of this integration method we calculated the volume of several free-electron spheres in this way and compared them with the exact values. We found that the ratio of the error in the volume, Δv, to the volume of the sphere, v, is given by the approximate formula

$$\frac{\Delta v}{v}\times\begin{pmatrix}\text{number of radii used}\\ \text{in volume calculation}\end{pmatrix}\approx 8.0.$$

Since we calculated 26 066 radii for the constant energy surfaces discussed in this work, we feel that the volumes that we have calculated (and hence the integrated densities of states) are accurate to about four decimal places.

PHYSICAL REVIEW VOLUME 161, NUMBER 3 15 SEPTEMBER 1967

Recovery of Electron-Irradiated Aluminum and Aluminum Alloys. I. Stage I

A. SOSIN
North American Aviation Science Center, Thousand Oaks, California

AND

K. R. GARR*
Atomics International, Division of North American Aviation, Incorporated, Canoga Park, California

(Received 28 April 1967)

The recovery in Stage I of the increase in electrical resistivity due to electron bombardment of aluminum has been examined using a "ratio-plot" technique. The differences in annealing between two samples with either different pre-irradiation histories or varying irradiation conditions are emphasized by this technique. Using samples irradiated to different doses (i.e., different initial defect concentration), the temperature region of non-first-order processes is clearly delineated; this region encompasses free interstitial migration. Using samples with 0.1 at.% copper or zinc and comparing with pure aluminum, the suppression of recovery by impurity doping is shown to be consistent with previous doping studies.

I. INTRODUCTION

THE Stage-I region (typically <70°K) is of central importance in the annealing of many irradiated metals as approximately 80–90% of the radiation-induced damage may be eliminated below 70°K, following electron irradiation near liquid-helium temperature (4.2°K). The first detailed studies of the Stage-I recovery following electron irradiation were performed by the General Electric group,[1] using copper. They reported five substages, labeled I_A through I_E, in increasing order of temperature. The first three of these substages were reported to follow first-order kinetics and were attributed to close-pair vacancy-interstitial annihilation. The fourth and fifth (I_D and I_E) were reported to possess the same activation energy. No simple chemical rate-theory formulation was found to adequately describe the I_D-I_E recovery. Corbett *et al.*[1] fitted their data to a diffusion model in which this region of recovery was ascribed to the migration of interstitials, characterized by its free migration energy, first to nearby vacant sites but later to more distant vacancies as continuing interstitial migration results in reduced spatial correlation between an interstitial and its original vacant site. The fact that complete recovery was not effected in this way was explained by further introduc-

* Work supported by the Division of Research, Metallurgy and Materials Programs, U. S. Atomic Energy Commission, under Contract No. AT(04-3)-701.

[1] J. W. Corbett, R. B. Smith, and R. M. Walker, Phys. Rev. 114, 1452 (1959); 114, 1560 (1959).